

UC Berkeley

UC Berkeley Previously Published Works

Title

23% efficient n-type crystalline silicon solar cells with passivated partial rear contacts

Permalink

<https://escholarship.org/uc/item/8mv2j23p>

Authors

Bullock, James

Wan, Yimao

Zhaoran, Xu

et al.

Publication Date

2018-06-15

DOI

10.1109/pvsc.2018.8547414

Peer reviewed

23% n-type crystalline silicon solar cells with $\text{TiO}_x / \text{LiF}_x / \text{Al}$ partial rear contacts

James Bullock¹, Yimao Wan^{1,2}, Xu Zhaoran¹, Di Yan², Pheng Phang², Mark Hettick¹, Chris Sumandsett², Ziv Hameiri³, Andres Cuevas² and Ali Javey¹

¹ Department of Electrical Engineering and Computer Sciences, University of California, Berkeley, California 94720, USA

² Research School of Engineering, The Australian National University (ANU), Canberra, Australian Capital Territory 2602, Australia.

³ School of Photovoltaic and Renewable Energy Engineering, University of New South Wales (UNSW), Sydney, NSW 2052, Australia

Abstract — Over the past 5 years there has been a significant increase in both the intensity of research and the performance of crystalline silicon (c-Si) devices which utilize metal compound selective contacts. Here we present a new $\text{TiO}_x / \text{LiF}_x / \text{Al}$ heterocontact stack which is implemented in high efficiency n-type cells as a partial rear contact without the need for heavy phosphorus doping. An efficiency of 23% is attained for this cell structure, setting a new benchmark for cells with dopant-free partial rear contacts. In addition, the performance of the cell is maintained after a short anneal at 400°C, suggesting its compatibility with conventional passivation activation anneals.

I. Introduction

Driven by a need to improve the crystalline silicon (c-Si) photovoltaic cost-to-performance ratio, recent years have seen a significant increase in the development of specialized heterocontacts for high efficiency c-Si solar cells. A sub-category of such heterocontacts is those which employ materials such as metal oxides and fluorides to selectively extract either electrons [1]–[3], or holes [4]–[7]. Some of these newly developed heterocontacts have enabled novel architectures, for example, n-type c-Si cells with dopant-free partial rear contacts (PRC), as depicted in the inset of Figure 1. This structure requires no heavy phosphorus doping – an ability which was not previously possible due the difficulties of directly contacting lowly doped n-type silicon.

As shown in Figure 1, the first successful demonstration of an n-type cell with a dopant free PRC employed a low work function ($\sim 3\text{eV}$) LiF_x / Al electrode [3]. This cell attained an

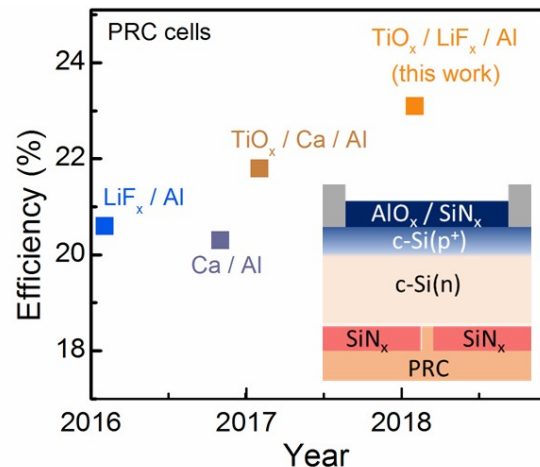


Figure 1: Efficiency progression of n-type c-Si solar cells with dopant-free PRCs. Inset shows the typical structure of such cells.

PRC cells with a similar efficiency of 20.3% [9]. In both of these initial cases, recombination at the PRC was estimated to be high, with an SRV of 5000 cm/s predicted for LiF_x / Al and likely higher for Ca / Al . The next evolutionary step in this cell structure was the integration of a passivation layer at the PRC interface. This came with the introduction of a $\text{TiO}_x / \text{Ca} / \text{Al}$ contact [10], which was found to provide both moderate passivation and low resistivity enabling an open circuit voltage V_{oc} and fill factor FF of 681 mV and 80.9% resulting in a large increase in the benchmark efficiency to 21.8%. Despite this significant increase in cell performance there still exist several possible avenues with which to easily improve this concept further. The most

prominent potential improvements are the rear reflection and the thermal stability of the structure.

This paper introduces the next iteration in this family of cells which targets the abovementioned issues. A novel $\text{TiO}_x / \text{LiF}_x / \text{Al}$ heterocontact is developed and integrated as a PRC. Unlike other low work function electrodes such as Ca and Mg, LiF_x / Al can act as a good rear reflector, increasing the possible short circuit current J_{sc} of the solar cell. In addition, the use of TiO_x , increases the thermal stability of the heterocontact introducing potential synergies with higher temperature processing steps. These two improvements allow the fabrication of a c-Si cell featuring a dopant free PRC which achieves a conversion efficiency of $\sim 23\%$ and exhibits thermal stability up to 400°C .

II. Contact Optimization

To initially assess the performance of the $\text{TiO}_x / \text{LiF}_x / \text{Al}$ heterocontact a series of contact resistivity and contact recombination test structures are fabricated.

Contact resistivity samples are fabricated on $\sim 1 \Omega\text{cm}$, FZ (100), n-type wafers. These are subjected to standard RCA cleaning and dilute ($\sim 5\%$) HF dips immediately prior to deposition of the heterocontact. The TiO_x layer is deposited via atomic layer deposition (ALD) at a chamber wall temperature of 230°C , using alternating cycles of Titanium tetraisopropoxide (TTIP) and water. Three sets of samples with TiO_x layers of 1.5, 3 and 6 nm are trialed to investigate the influence of TiO_x thickness. Following this, a LiF_x ($\sim 1 \text{ nm}$) / Al ($\sim 200 \text{ nm}$) stack is deposited via thermal evaporation through a shadow mask to define a transfer-length- method (TLM) pattern. It should be noted that the accuracy of the TLM approach is compromised when applied to moderate or

high resistivity wafers, as is the case here. Figure 2 shows the extracted contact resistivity ρ_c as a function of annealing temperature for the three different TiO_x thicknesses. Annealing was performed using sequential 10 minute anneals between 100°C and 300°C by placing samples directly on a hotplate in air. It can be seen in the as-deposited (25°C) state that ρ_c increases with the thickness of the TiO_x , suggesting that the bulk resistivity of the TiO_x could be limiting the total contact resistivity. Interestingly, with increasing anneal temperature, a clear decrease in ρ_c occurs for all three thicknesses. The origin of this reduction is still under investigation but could be associated with a reduction of the TiO_x layer, as suggested in other studies [2], [10], or an interaction between LiF_x and TiO_x . Regardless of the mechanism, the results suggest that annealing the contacts at low temperatures can lead to a significant reduction in ρ_c .

As a complimenting set of information, the surface recombination velocity (SRV) at the $\text{TiO}_x / \text{c-Si}$ interface is extracted via carrier lifetime samples measured by photoconductive decay (PCD). These samples were also prepared on $\sim 1 \Omega\text{cm}$, FZ (100), n-type wafers and subjected to standard RCA cleaning and HF dips. To form the symmetrical lifetime samples TiO_x layers were deposited on either side with thicknesses of 1.5, 3 and 6 nm. The measured excess carrier dependent carrier lifetime is presented in Figure 2b showing an increase in lifetime with increasing thickness. Included in the same plot are upper limit SRV values, extracted assuming an infinite bulk lifetime, at an excess carrier density of 10^{15} cm^{-3} . The decreasing SRV shows that the surface recombination may be reduced by increasing the TiO_x thickness - a factor which must be balanced against the ρ_c behavior of Figure 2a. It should be noted that these SRV values are likely to increase after deposition of

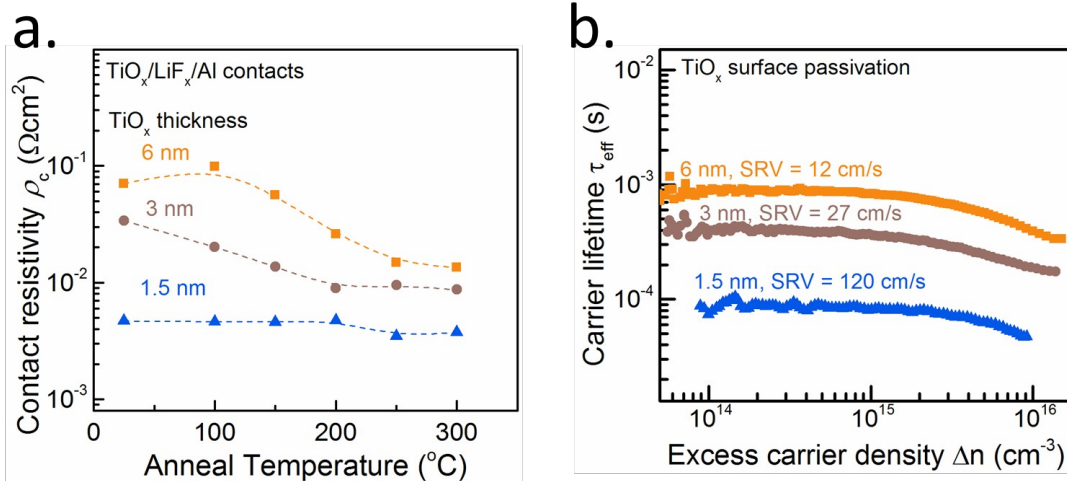


Figure 2: **a.** contact resistivity of $\text{TiO}_x / \text{LiF}_x / \text{Al}$ contacts on n-type $1 \Omega\text{cm}$ c-Si as a function of anneal temperature for different TiO_x thicknesses; **b.** minority carrier lifetime as a function of excess carrier density for n-type $1 \Omega\text{cm}$ c-Si wafers passivated with different TiO_x thicknesses. Also listed for each thickness is the SRV, extracted at 10^{15} cm^{-3} assuming an infinite bulk lifetime.

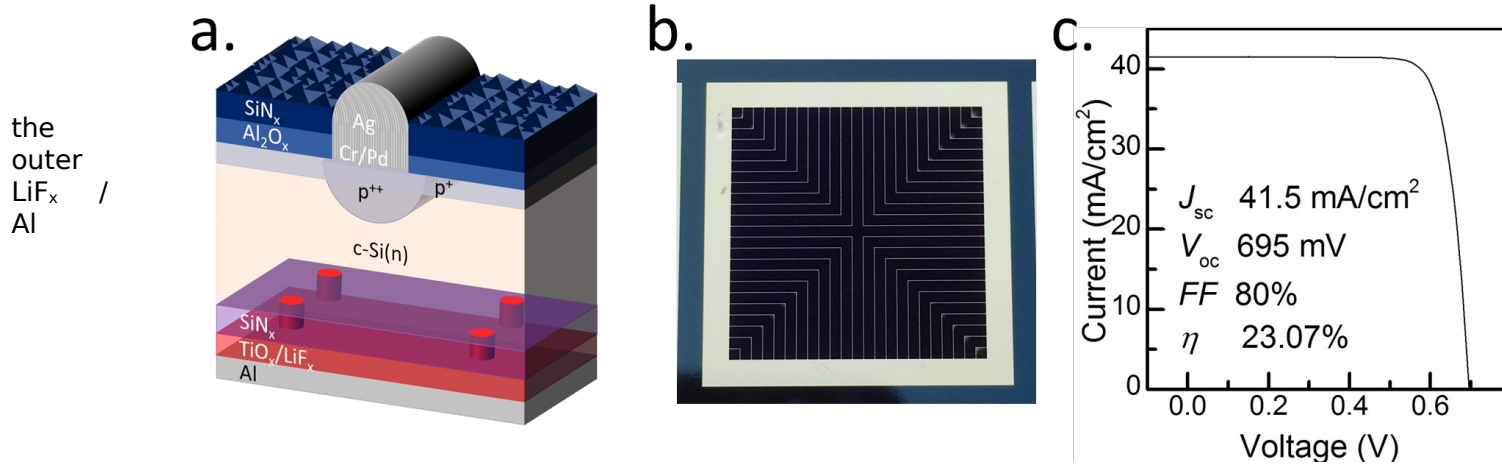


Figure 3: **a.** cross sectional schematic, **b.** micrograph of front surface and **c.** measured 1-sun J/V of the n-type cell with TiO_x / LiF_x / Al PRCs presented in this work.

contact and thermal annealing and hence should be used as a guide only.

As the target of this study is to implement such a contact as a 1% fraction PRC, we conclude that only the combination of TiO_x (1.5 nm) / LiF_x / Al is appropriate owing to the strict requirement of mΩcm² scale contact in such a design. An additional possibility, not explored here, is to use the thicker TiO_x combinations as full-area rear contacts.

III. Cell Optimization

The previously described PRC is tested by integrating it into an n-type cell with an optimized front-side, the cross-sectional structure of which is depicted in Figure 3a. This cell is fabricated with a double boron diffusion on the front to create localized heavily doped p⁺⁺ regions under the direct metal contacts. The front contacts only take up 1-2% of the front surface, a micrograph of the cells front contact pattern is shown in Figure 3b. An AlO_x / SiN_x passivation and antireflection stack is deposited in the front non-contacted regions. A rear side SiN_x passivation / dielectric spacer is patterned with small 30 μm diameter holes to the c-Si surface covering less than 1% of the rear surface area. Through these holes the TiO_x (1.5nm) / LiF_x / Al stack directly contacts the n-type c-Si surface forming the PRC. Following fabrication, the whole cell structure is annealed at 350°C for 30 minutes in forming gas (5% H₂, 95% N₂). This anneal step was found to result in the highest FF without impacting the V_{oc} .

Figure 3c shows the obtained light current density - voltage (J/V) plot of the champion cell, measured under standard 1-Sun conditions (100mW/cm², 25°C, AM 1.5G spectrum) showing a conversion efficiency of 23.1% has been achieved—the highest value for this cell class to date. The obtained FF and V_{oc} of 80% and 696 mV suggest that low ρ_c has been attained and some level of surface recombination suppression has been maintained at the heterocontact after the anneal. Perhaps the most impressive parameter is the J_{sc} , reaching 41.5 mA/cm². This value, which was also measured by external quantum efficiency analysis at 41.4 mA/cm², falls just below the maximum expected for such a structure, after accounting for thicknesses, contact fractions and materials. It is important to note that in comparison to previous n-type cells with dopant free PRCs, the above presented cell also benefits from significant optimization of other cell regions. This is evidenced by the very high J_{sc} which stems, in part, from a near perfect front side design.

To investigate the stability of the contact, cells were further annealed at 400°C for 10 minutes in forming gas, resulting in no significant change in overall cell performance (a slight drop in V_{oc} was compensated by a slight increase in FF). This suggests the compatibility of this contact structure with conventional FGA steps utilized for surface passivation.

IV. Ongoing work

In addition to the results presented here, we are currently working on improving our understanding of the contact activation process via materials based characterization of the TiO_x / LiF_x / Al stack. These results will be presented, along with a more detailed champion cell

characterization and modelling section, at the IEEE PVSC.

V. Conclusion

In this study we have introduced the next iteration in a fast improving family of n-type solar cells featuring dopant-free partial rear contacts. In doing so we have set a new benchmark for efficiency and stability. To achieve this a $\text{TiO}_x / \text{LiF}_x / \text{Al}$ contact is developed which is 'activated' at temperatures of $\sim 300^\circ\text{C}$ to provide a low resistance contact to moderately doped n-type surfaces. This is integrated into an optimized n-type PRC cell with an efficiency of $\sim 23\%$, the highest for this architecture to date. The same structure is found also to be resilient to short anneals at 400°C in forming gas, suggesting its compatibility with standard passivation anneal steps.

References

- [1] S. Avasthi, W. E. McClain, G. Man, A. Kahn, J. Schwartz, and J. C. Sturm, "Hole-blocking titanium-oxide/silicon heterojunction and its application to photovoltaics," *Appl. Phys. Lett.*, vol. 102, no. 20, p. 203901, 2013.
- [2] X. Yang, K. Weber, Z. Hameiri, and S. De Wolf, "Industrially feasible, dopant-free, carrier-selective contacts for high-efficiency silicon solar cells," *Prog. Photovolt. Res. Appl.*, vol. 25, no. 11, pp. 896–904, Nov. 2017.
- [3] J. Bullock *et al.*, "Efficient silicon solar cells with dopant-free asymmetric heterocontacts," *Nat. Energy*, vol. 1, no. 1, p. 15031, 2016.
- [4] C. Battaglia *et al.*, "Hole Selective MoO_x Contact for Silicon Solar Cells," *Nano Lett.*, vol. 14, no. 2, pp. 967–971, 2014.
- [5] J. Geissbühler *et al.*, "22.5% efficient silicon heterojunction solar cell with molybdenum oxide hole collector," *Appl. Phys. Lett.*, vol. 107, no. 8, p. 081601, 2015.
- [6] M. Bivour, J. Temmler, H. Steinkemper, and M. Hermle, "Molybdenum and tungsten oxide: High work function wide band gap contact materials for hole selective contacts of silicon solar cells," *Sol. Energy Mater. Sol. Cells*, vol. 142, pp. 34–41, Nov. 2015.
- [7] G. Masmitjà *et al.*, " V_2O_x -based hole-selective contacts for c-Si interdigitated back-contacted solar cells," *J. Mater. Chem. A*, vol. 5, no. 19, pp. 9182–9189, May 2017.
- [8] J. Bullock *et al.*, "Lithium Fluoride Based Electron Contacts for High Efficiency n-Type Crystalline Silicon Solar Cells," *Adv. Energy Mater.*, vol. 6, no. 14, p. 1600241, Jul. 2016.
- [9] T. G. Allen *et al.*, "Calcium contacts to n-type crystalline silicon solar cells," *Prog. Photovolt. Res. Appl.*, p. n/a-n/a, Jan. 2016.
- [10] T. G. Allen *et al.*, "A Low Resistance Calcium/Reduced Titania Passivated Contact for High Efficiency Crystalline Silicon Solar Cells," *Adv. Energy Mater.*, vol. 7, no. 12, p. 1602606, Feb. 2017.